

Energy level alignment at interfaces of organic semiconductor heterostructures

I. G. Hill^{a)} and A. Kahn

Department of Electrical Engineering, Princeton University, Princeton, New Jersey 08544

(Received 3 June 1998; accepted for publication 20 August 1998)

We have used ultraviolet photoelectron spectroscopy (UPS) to investigate the interfaces of two organic semiconductor heterostructures. UPS was used to determine the relative energies of the highest occupied molecular orbitals of the organic semiconductors, and to measure the interface dipoles at each interface. The two systems studied were the 4-4'-*N,N'*-dicarbazolyl-biphenyl(CBP)/tris(8-hydroxy-quinoline)aluminum (Alq₃) interface, and the copper phthalocyanine (CuPc)/*N,N'*-diphenyl-*N,N'*-bis(1-naphthyl)-1,1'-biphenyl-4,4''diamine (α -NPD) interface. The assumption of a common vacuum level was found to be valid, within experimental uncertainty, for both interfaces. © 1998 American Institute of Physics.

[S0021-8979(98)05222-0]

I. INTRODUCTION

Organic light emitting devices (OLEDs) can be fabricated using small-molecule organic semiconductors deposited in vacuum on a wide variety of substrates.¹ This class of materials may lead to the manufacturing of inexpensive large-area displays, and much work has therefore been devoted to improving device structures and understanding their operation. The simplest OLED structure consists of a single layer of organic material between two metallic contacts. One contact is responsible for hole injection, while the other injects electrons. The hole injecting electrode (anode) is usually indium tin oxide (ITO) deposited on glass, which is transparent to the emitted light. These devices are inherently inefficient due to unbalanced injection of carriers, leading to a large fraction of one of the charge carriers traversing the device without combining to form excitons. Furthermore, recombination in these devices typically occurs near the electrode which injects the lower mobility charge carrier.² Excitons formed near an electrode have an enhanced probability of decaying via a nonradiative path due to their dipole interaction with the metallic electrode. These nonradiative recombinations further decrease the quantum efficiency of the device.

The performance of the single layer structure can be improved upon through the addition of a second organic layer. Double layer devices consist of an electron transport layer (ETL), and a hole transport layer (HTL), one of which also acts as the emissive layer.³ The interface between the ETL and HTL may create barriers to hole or electron transport, depending on the relative energies of the levels. Ideally, carriers are confined at the interface by such a barrier within the emissive layer, while the other type of carriers are freely injected into this layer. The advantages of this scheme are twofold: the flexibility added by a second organic layer allows a better balance of electron and hole injection; and the recombination zone is moved away from the metal electrode,

enhancing the probability of radiative exciton recombination when compared to a single layer structure.

In this scheme, it is obviously important to be able to predict the relative energies of the highest occupied molecular orbitals (HOMO), and lowest unoccupied molecular orbitals (LUMO) of the two organics at the interface. It is usually assumed that the vacuum levels of the two materials align at the interface.⁴ The Fermi levels of the two materials are required to align in thermal equilibrium. The weak van der Waals intermolecular bonding between organic semiconductors is not expected to result in a large density of gap states, and the Fermi level should therefore move freely at organic heterostructure interfaces, thus allowing the vacuum levels to align. The barrier to hole (electron) injection from material *A* into material *B* is given by $IE_B - IE_A(EA_A - EA_B)$, where *IE* is the ionization energy of the material, defined as the energy difference between the vacuum level and the low binding energy edge of the HOMO, and *EA* is the electron affinity, defined as the energy difference between the vacuum level and the high binding energy edge of the LUMO. A positive barrier is blocking, and a negative or zero barrier passes carriers. It has been well documented that the assumption of vacuum level alignment at metal/organic interfaces is not valid,⁵⁻¹¹ thus prompting careful examination of the electronic structure of a number of organic semiconductor heterojunctions. Using UPS, we have measured the barriers to hole injection, and the magnitude of the interface dipole (vacuum level shift), at two organic/organic interfaces: CBP/Alq₃ and α -NPD/CuPc. CBP, an aromatic diamine, has been recently shown to enhance electron injection from nonoxidizing metals like Ag, prompting interest in the investigation of interfaces between CBP and electron transport materials, such as Alq₃, for use in the cathode side of OLEDs. Similarly, CuPc in contact with α -NPD was recently introduced in nonmetal contact OLEDs.⁴ Transport across these interfaces is central to the analysis of device efficiency and requires a detailed understanding of their electronic structure.

^{a)}Corresponding author; electronic mail: ianhill@ee.princeton.edu

II. EXPERIMENT

All measurements and depositions were performed in an ultrahigh vacuum system (base pressure 2×10^{-10} Torr), consisting of a main analysis chamber and a sample preparation chamber. The analysis chamber was equipped with an x-ray source (Al and Zr anodes), a He discharge lamp, and a double-pass cylindrical mirror analyzer. The resolution of the UPS system was ≈ 150 meV, determined from the width of the Fermi level observed on polycrystalline Au.

The organic materials were purified *ex situ* by several cycles of gradient sublimation, and were thoroughly degassed after being placed in the UHV preparation chamber. Organic thin films were deposited from heated effusion cells at rates ranging from 5 to 20 Å/min. The pressure during organic depositions was $\leq 10^{-9}$ Torr. All thicknesses were determined by timed depositions calibrated using a quartz crystal microbalance. No correction was made for sticking coefficients. The substrates used for all samples were thick gold films deposited on Si(100) wafers. All depositions were performed at room temperature.

Samples were prepared by depositing a base organic (≈ 100 Å) film on a substrate. This surface was studied using ultraviolet photoelectron spectroscopy (UPS), to determine the position of the vacuum level, the IE and the HOMO position relative to the Fermi level. The position of the vacuum level in the spectra is determined by adding the photon energy to the kinetic energy of the low energy secondary electron cutoff collected with the sample at a negative bias (-3 V) to overcome the contact potential between the sample and detector. The lowest energy secondary electrons emerge from the sample at the vacuum level. A hypothetical electron originating at the vacuum, photoexcited by the same photon energy, would therefore have a kinetic energy one photon energy above that of the lowest energy secondary electrons. These parameters, as well as the shape of the photoemission spectra were used to assess the quality of the films. Organic overlayers were then deposited on the original film. UPS spectra were collected as a function of the overlayer thickness to determine the vacuum level shift, the relative positions of the two HOMOs, and to study the evolution of the spectral shape.

III. RESULTS

A. CBP/Alq₃ interface

CBP was deposited on the clean Alq₃ film. A summary of the data collected as a function of CBP thickness is shown in Fig. 1. The lowest spectrum in Fig. 1 is characteristic of bulk Alq₃.¹² The HOMO is identified as the peak ≈ 3 eV below the Fermi level. The top of the HOMO is estimated by linear extrapolation of the low binding energy side of the peak to be at 2.1 ± 0.1 eV below the Fermi level. Using the onset of photoemission to obtain the vacuum level, one finds $IE = 6.1 \pm 0.1$ eV, which is in reasonable agreement with previous studies.¹³

The spectral features evolve, becoming more CBP-like with increasing CBP thickness. The enlargement of the HOMO region in Fig. 3 demonstrates that the Alq₃ features do not shift in energy as a function of CBP deposition. With

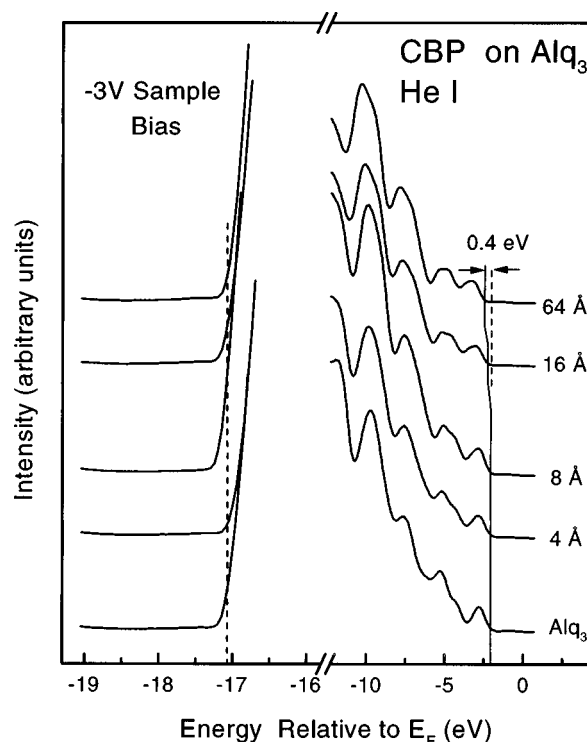


FIG. 1. He I UPS spectra for the CBP deposited on Alq₃ system. The bottom spectrum was collected from the clean Alq₃ surface. The 64 Å spectrum is characteristic of bulk CBP.

64 Å CBP, the Alq₃ features are completely suppressed, and the spectrum is indicative of bulk CBP.¹¹ The calculation of the IE yields 6.5 ± 0.1 eV, again in reasonable agreement with previous studies.¹¹ The top of the HOMO of the CBP is found at 0.4 ± 0.1 eV higher binding energy than that of the Alq₃, indicating that the barrier to hole injection from Alq₃ to CBP is 0.4 ± 0.1 eV. It is difficult to unambiguously identify the lowest binding energy feature in the 64 Å spectrum as containing no contribution from Alq₃, because of the similar shapes and overlapping energy ranges of the HOMO features of these two organics. To verify our conclusions, the difference in binding energies between the top of this feature and the peak of the intense feature ≈ 10.3 eV below the Fermi level was compared to previous studies of CBP,¹¹ and found to agree within < 0.1 eV, which is our experimental uncertainty. Estimating the relative positions of the LUMOs using the optical gaps of CBP and Alq₃ (3.1 and 2.7 eV, respectively^{11,12}), leads to levels which are aligned, ± 0.1 eV, indicating that the barrier to electron injection between these two materials is negligible. A slight increase in the position of the vacuum level is found after deposition of CBP on Alq₃, indicating the formation of a small interface dipole, with negative charge transferred from the Alq₃ to the CBP. The magnitude of the vacuum level shift, however, is only 100 meV, which is less than the uncertainty in this measurement.

B. α -NPD/CuPc interface

The formation of the α -NPD/CuPc interface was studied by depositing α -NPD on an initially clean 100 Å thick CuPc

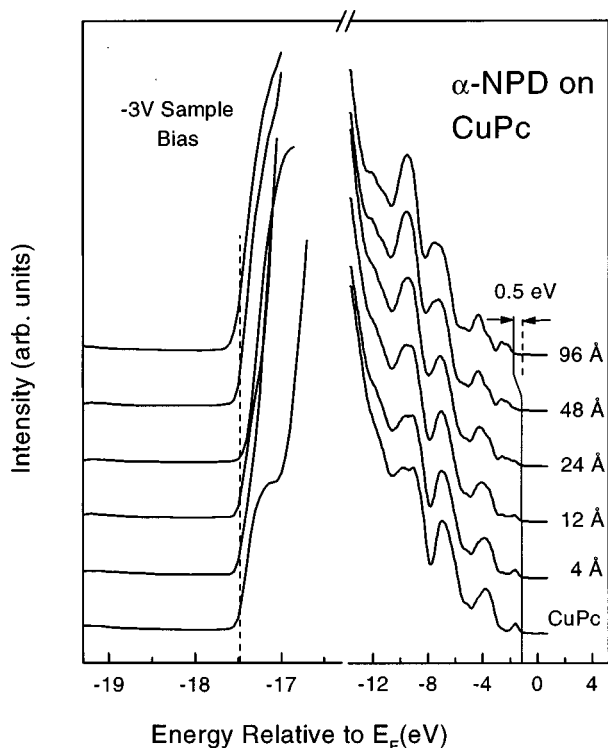


FIG. 2. Same as Fig. 1, for NPD deposited on CuPc.

film. The data are summarized in Fig. 2. The top of the CuPc HOMO is 1.3 ± 0.1 eV below the Fermi level. Using the onset of photoemission yields an IE of 5.0 ± 0.1 eV. The deposition of α -NPD results in spectra containing both CuPc and α -NPD features. The α -NPD HOMO is identified as the feature which peaks at ≈ 2 eV below the Fermi level. This feature, and a second ≈ 2.8 eV below the Fermi level, are well separated from the CuPc HOMO, and can clearly be seen to evolve with increasing α -NPD thickness. At 48 Å, the CuPc HOMO can still be seen, indicating incomplete α -NPD coverage of the surface, since this thickness is much greater than the experimental probing depth of ≈ 10 Å. This may indicate that the α -NPD forms three-dimensional islands separated by regions of bare CuPc, or that the sticking coefficient is significantly less than unity. At 96 Å nominal coverage, the CuPc features are fully suppressed, and the spectrum corresponds to bulk α -NPD. The enlargement of the HOMO in Fig. 3 shows that the CuPc energy levels do not shift by any significant amount as a function of α -NPD deposition, at least up to a coverage of 48 Å. The top of the α -NPD HOMO is found at 0.5 ± 0.1 eV below that of the CuPc, giving an equivalent barrier for hole injection from CuPc to α -NPD. No measurable shift of the vacuum level is found, indicating that the dipole shift at the interface must be < 100 meV.

IV. DISCUSSION

Fig. 4 includes molecular level offset diagrams for the Alq_3/CBP and $\text{CuPc}/\alpha\text{-NPD}$ interfaces derived from the data described in the preceding section. It should be noted that the HOMO offsets and vacuum level shifts reported here are the results of direct measurements which are not affected by the 0.2–0.3 eV variations reported for the IEs of the films. The

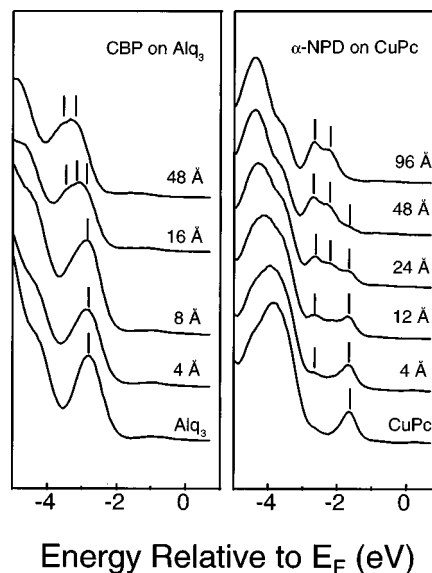


FIG. 3. Enlargement of the spectra from Figs. 1 and 2 showing the evolution of the HOMO.

accuracy and repeatability of the measurements are of the order of 150 meV. The two heterojunctions investigated here were recently used in heterojunction OLEDs and their HOMO and LUMO offsets are therefore particularly relevant to the behavior of these devices. CuPc was used as an intermediate layer to improve the hole injection from indium tin oxide to α -NPD. It is interesting to note that the theoretical HOMO offset based on the principle of E_{vac} alignment and on previously published CuPc and α -NPD IEs (Refs. 12 and 14) was 0.9 eV, too large a barrier to allow normal operation of the device. Our measurements demonstrate that the barrier is in fact nearly half of the theoretical barrier, making CuPc an acceptable ‘‘ladder step’’ between ITO and α -NPD.

CBP was recently used as an intermediate layer to allow efficient electron injection between Ag and Alq_3 . We have already demonstrated that the Ag/CBP electron injection barrier is ≈ 0.6 eV.¹¹ It is possible that the 0.4 eV offset between the HOMOs of the Alq_3 and CBP blocks holes at the interface, preventing them from reaching the cathode. This scenario may improve device performance in two ways. Preventing holes from reaching the cathode will increase the percentage of holes which form excitons, thereby increasing

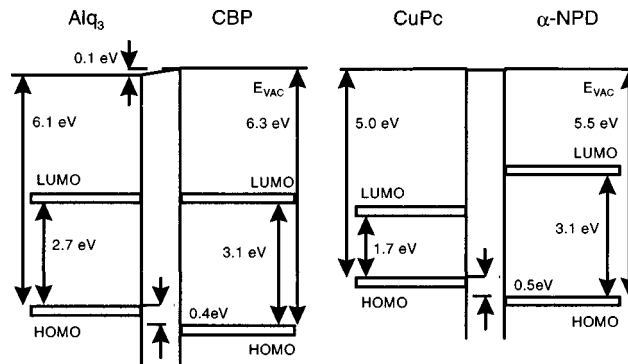


FIG. 4. Molecular level diagrams constructed from the data in Figs. 1 and 2.

the recombination efficiency. Second, an accumulation of positive charge at the Alq₃/CBP interface will increase the electric field within the CBP layer. If this field exceeds a critical threshold, electron tunneling from the Ag into the CBP will exceed thermionic injection, leading to a much lower "effective" injection barrier. This possibility is currently being investigated and will be presented at a later time. In any case, the present measurement suggests that the CBP and Alq₃ LUMOs are aligned at the interface, thus making the injection of electrons from CBP into Alq₃ particularly easy.

Unlike metal/organic interfaces,^{5,6,8-10} where the assumption of a common vacuum level at the interface breaks down, the majority of the organic/organic heterostructures considered here can be accurately modeled using vacuum level alignment. Only the PTCDA/Alq₃ and Alq₃/ α -NPD interfaces have been found to have an interface dipole which is larger than the ± 150 meV uncertainty in our measurements.¹² This observation can be rationalized by noting that the intermolecular forces within these van der Waals solids and at interfaces are weak, and one would therefore not expect any significant interaction between neighboring molecules, even of dissimilar species. Partial charge transfer between molecular species, and therefore interface dipoles, is not expected. At organic/metal interfaces, however, chemical interactions between metal atoms and molecules do occur. These interactions may be seen as resulting in partial charge transfer, which is responsible for the interface dipole, or as creating states within the organic semiconductor gap, which limit the range over which the Fermi level can move.¹⁵ By and large, organic-organic heterojunctions are therefore closer to the noninteracting systems idealized by the Anderson model, although deviations marked by interface dipoles can occur at heterojunctions between organics with widely different IEs and EAs such as PTCDA and Alq₃.¹³

V. CONCLUSION

Using UPS we have measured the HOMO offsets, and inferred electron and hole barriers at the interfaces between

CBP and Alq₃, as well as α -NPD and CuPc. The assumption of vacuum level alignment at these interfaces was found to be valid within experimental uncertainties. The molecular level offsets determined in this work contribute to the understanding of the transport behavior in recently fabricated OLEDs.

ACKNOWLEDGMENTS

Support of this work by the MRSEC program of the National Science Foundation (Award No. DMR-9400362) and by the New Jersey Center for Optoelectronics (Grant No. 97-2890-051-17) is gratefully acknowledged. One of the authors, I.H., acknowledges the support of NSERC of Canada. The authors also thank D. O'Brien and G. Parasarathy for useful discussions, and the group of S. R. Forrest for providing the purified Alq₃, α -NPD and CuPc, and D. E. Loy and M. T. Thompson for providing the CBP.

¹S. R. Forrest, *Chem. Rev.* **97**, 1793 (1997).

²B. K. Crone, P. S. Davids, I. H. Campbell, and D. L. Smith, *J. Appl. Phys.* **84**, 833 (1998).

³C. W. Tang and S. A. Van Slyke, *Appl. Phys. Lett.* **51**, 913 (1987).

⁴G. Parthasarathy, P. E. Burrows, V. Khalfin, V. G. Kozlov, and S. R. Forrest, *Appl. Phys. Lett.* **72**, 2138 (1998).

⁵H. Ishii and K. Seki, *IEEE Trans. Electron Devices* **44**, 1295 (1997).

⁶A. Rajagopal and A. Kahn, *J. Appl. Phys.* **84**, 355 (1998).

⁷Y. Hirose and A. Kahn, *Appl. Phys. Lett.* **68**, 217 (1996).

⁸Y. Hirose, C. I. Wu, V. Aristov, P. Soukiassian, and A. Kahn, *Appl. Surf. Sci.* **113/114**, 291 (1997).

⁹Y. Hirose, A. Kahn, V. Aristov, P. Soukiassian, V. Bulovic, and S. R. Forrest, *Phys. Rev. B* **54**, 13 748 (1996).

¹⁰K. Sugiyama, D. Yoshimura, E. Ito, T. Miyazaki, Y. Hamatani, I. Kawamoto, H. Ishii, Y. Ouchi, and K. Seki, *Synth. Met.* **86**, 2425 (1997).

¹¹I. G. Hill, A. Rajagopal, and A. Kahn, *J. Appl. Phys.* **84**, 3236 (1998).

¹²A. Rajagopal and A. Kahn, *J. Appl. Phys.* **83**, 2649 (1998).

¹³A. Rajagopal and A. Kahn, *Adv. Mater.* **10**, 140 (1998).

¹⁴K. Seki, *Mol. Cryst. Liq. Cryst.* **171**, 255 (1989).

¹⁵I. G. Hill, A. Rajagopal, A. Kahn, and Y. Hu, *Appl. Phys. Lett.* **73**, 662 (1998).